Bitlis Eren Üniversitesi Fen Bilimleri Dergisi
BİTLİS EREN UNIVERSITY JOURNAL OF SCIENCE
ISSN: 2147-3129/e-ISSN: 2147-3188
VOLUME: 13 NO: 4 PAGE: 1147-1157 YEAR: 2024
DOI: 10.17798/bitlisfen.1521704

Performance Evaluation of the Time-Frequency Transformation Methods on Electrical Machinery Fault Detection

Mehmet Emin KILIC[1], Yunus Emre ACAR[2*]

[1]*Hey Teknoloji, Kahramanmaras, Türkiye*
[2]*Selcuk University, Faculty of Technology, Department of Electrical and Electronics Engineering, Konya, Türkiye*
(ORCID: 0009-0003-2381-7873) (ORCID: 0000-0002-6809-9006)

Keywords: Fault Detection, Machine Learning, Predictive Maintenance, Time-Frequency Transform, Transfer Learning, Vibration.

Abstract

Detecting faults in electrical machine systems is crucial for developing maintenance strategies. Modern technology enables personalized maintenance planning for system components by continuously or periodically monitoring systems with sensors. The first step in condition-based maintenance planning is predicting faults from sensor data. Monitoring vibration signals is one of the most preferred approaches for fault diagnosis in electrical machine systems. We have used a dataset containing vibration data recorded to detect intentionally created faults in an electrical machine system. The paper spots three popular methods to convert the time domain data into the frequency domain: power spectral density signal, spectrogram images, and scalogram images. Furthermore, we have analyzed the performance of the popular machine learning and deep learning methods with frequency-domain inputs. We have reported the results with accepted performance metrics such as accuracy, precision, recall, and F1 score. Our findings indicate that spectrogram images with the InceptionV3 model achieve maximum accuracy of over 98% accuracy among. The findings also highlight the necessity of carefully selecting model parameters based on the data type.

1. Introduction

Electric machine systems are among the most crucial components of the industry and hold a pivotal position in manufacturing facilities [1]. Faults or unplanned downtime in electric machine systems can lead to extensive financial consequences and damage to the reputation of facilities [2]. Consequently, developing maintenance strategies for electric machine systems becomes beneficial and imperative. While academic studies categorize maintenance strategies in various ways, many researchers unanimously agree on dividing maintenance activities into three fundamental groups: corrective, preventive, and predictive maintenance [3-5].

Corrective maintenance, which emphasizes post-failure recovery, and preventive maintenance, which aims to prevent potential failures before they occur, represent traditional approaches. Since corrective maintenance requires intervention after a failure, it is preferred in areas where unplanned downtime is not critical and is tolerable. On the other hand, preventive maintenance, in facilities where continuity is crucial, deems postponing the failure to a more suitable time by taking overly precautious measures sufficient. This approach involves creating a periodic maintenance and repair plan considering the average lifespan of electric machine system components. However, inherent unpredictability remains a challenge for electric machine systems. Determining a precise timeframe for potential failure is difficult due to the numerous factors influencing the expected lifespan of system components [6]. This uncertainty often leads facilities to adopt cautious measures and rely on maintenance programs based on generalized service life. Selçuk [4] has elucidated that

*Corresponding author: yacar@selcuk.edu.tr
Received: 23.07.2024, Accepted: 04.10.2024

such overly precautionary measures, especially concerning personnel and spare parts inventories, often lead to economic inefficiencies.

In recent years, supported by technological advancements and the proliferation of sensor technology, predictive maintenance offers personalized maintenance programs for electric machine systems [7]. In this approach, sensors continuously monitor the health of the motor and promptly flag any abnormalities. Beyond mere detection, the aim is to evaluate the progression and criticality of abnormalities and then make informed decisions regarding appropriate maintenance or repair interventions.

Two primary techniques dominate predictive maintenance in electric machine systems: current-based and vibration-based methods. The former approach, as detailed by Niu et al. [8], relies on the analysis of the motor's current signal. On the other hand, the vibration-based approach utilizes strategically positioned sensors to identify types of faults that create a vibration signature [9]. While time-domain analyses have occasionally been employed in both techniques, many modern studies [10] support frequency spectrum analysis. Tools such as Fast Fourier Transform (FFT), Short-Time Fourier Transform (STFT), Wavelet Transform (WT), and Power Spectral Density (PSD) commonly feature prominently in these analyses.

Features derived from these analytical tools are then interpreted. Historically, expert judgments formed the basis of such interpretations. However, the emergence of complex computational techniques like fuzzy logic, artificial neural networks, machine learning, and deep learning has ushered in a new era of analysis [11]. Garcia et al. [12], outlining the main stages of the standard predictive maintenance process, have enumerated various stages ranging from continuous monitoring of motor health to the strategic preparation of maintenance and repair plans based on multiple determinants. The first step in predictive maintenance is the disaggregation of faults using current or vibration signatures. Predicting how each disaggregated fault will deteriorate over time constitutes the next step. Proposing specific maintenance and repair plans for the predicted types of faults represents the final step of the approach. This study sheds light on the classification stage of predictive maintenance, a critical intersection in a comprehensive process. Inspired by recent advancements, the applicability of machine learning and deep learning methodologies to detect mechanical abnormalities via vibration signatures of electric machines is discussed. To provide a holistic perspective, results from machine learning and deep learning models are presented using 1-D power spectral density and 2-D spectrogram and scalogram images.

2. Material and Method

The most encountered electrical faults are winding and rotor bar faults, while bearing faults, misalignment, and imbalance are the most prevalent mechanical issues. This article focuses on classifying the mechanical faults in electric machine systems using vibration signals.

2.1. Dataset

The Machine Fault Dataset, MaFaulDA [13], was utilized in the article. The experimental setup comprises a circular metal disk combined with a DC motor. By placing various weights onto the disc, the imbalance failure is simulated. The overall system contains two bearings: one placed between the motor and the disk and the other positioned at the end of the system after the disk. Throughout the remainder of the article, the locations of the bearings will be referred to as Location 1 and Location 2, respectively. The dataset includes radial, tangential, and axial vibration signals recorded from these locations. After analyzing the data, we decided to use only the vibration signals on the radial axis. The data for each experiment has a length of 250,000, with an observation period of 5 seconds and a sampling frequency of 50 kHz. The dataset contains six distinct classes of data, consisting of five fault conditions and one healthy condition. Descriptions of the dataset are tabulated in Table 1.

2.2. PSD

PSD is a powerful tool for analyzing the frequency spectrum of signals. It serves as a mathematical measure of the power distribution across frequencies and finds widespread use in various applications such as communication [14, 15], power systems [16], optics [17], and more. Since anomalies in electric motors manifest differently in the frequency spectrum, PSD is also beneficial for fault classification studies.

There are various PSD estimation methods, broadly classified as parametric and non-parametric. Parametric estimation techniques require modeling the system with a limited number of parameters using autoregressive, moving average, and autoregressive moving average models. The accuracy of estimation is directly proportional to the accuracy of the model created.

Table 1. The data amount for each class and dataset explanation.

Class	Number of Data	Explanation
Normal	49	The data set has been created by 49 distinct experiments with different rotational speeds varying between 737 rotations per minute (rpm) and 3686 rpm.
Imbalance	333	The imbalance cases are created by placing various weights from 6g to 35g on the disc. For 44 different rpm values, 333 experiments have been conducted.
Horizontal misalignment	197	Misalignments are created by horizontally shifting the motor shaft from 0.5mm to 2 mm over 197 experiments.
Vertical misalignment	301	Misalignments are created by vertically shifting the motor shaft 0.51 mm to 1.9 mm over 301 experiments.
Overhang	513	Deliberately damaged bearings (outer and inner track faults, rolling element faults) have been placed at Location 1 in the experiments.
Underhang	558	Deliberately damaged bearings (outer and inner track faults, rolling element faults) have been placed at Location 2 in the experiments.
Total	1951	

Moreover, as the data size increases, the complexity of the method also increases. On the other hand, non-parametric approaches like the periodogram are more flexible and do not require a model or prior information about the system. Hence, they are suitable for fault detection applications in electric machine systems with nonlinear characteristics and difficult-to-model behavior.

This study focuses on the non-parametric PSD estimation technique known as the Welch approach. The estimated PSD of the recorded vibration signals is utilized as input for deep learning methods.

Within the Welch approach, the signal is divided into K segments, each of length M, with the inclusion of a designated overlap ratio. Following this division, these segments undergo multiplication by a window function represented as $w(n)$. Utilizing a window jump size of R, the calculated weighted segments, designated as $x_m(n)$, are determined as outlined in (1).

$$x_m(n) \cong w(n)x(n+mR)$$
$$n = 0,1,2,\dots,M-1, m = 0,1,2,\dots,K-1 \quad (1)$$

Subsequent to this, the periodogram is derived through the computation of the square of the absolute value of the N-length Fourier transform applied to the divided segments. The periodograms for each segment are calculated as in (2).

$$P_{x_m,M(w_k)} \cong \frac{1}{M}\left|\sum_{n=0}^{N-1} x_m(n)e^{\frac{-j2\pi nk}{N}}\right|^2 \quad (2)$$

Finally, the periodograms of all subsegments are averaged to obtain the overall PSD to decrease the variance. The overall PSD, $\hat{S}_x^W(w_k)$, is evaluated as given in (3).

$$\hat{S}_x^W(w_k) \cong P_{x_m,M(w_k)} = \sum_{m=0}^{K-1} P_{x_m,M(w_k)} \quad (3)$$

Figure 1(a) and Figure 1 (b) depict sample PSD estimates obtained from vibration signals taken respectively from Location 1 and Location 2 for each class provided in Table 1. Figure 1(a) illustrates that different peak points occur at distinct frequencies for each class, reinforcing the idea that the PSD of vibration signals obtained from this point is beneficial to distinguish between different types of faults. However, as shown in Figure 1(b), the sensor at Location 2 exhibits a level of DC noise that complicates the direct use of the data.

2.3. Spectrogram

A spectrogram is a powerful tool that visually represents the dynamic frequency changes over time, commonly used in analyzing sound and vibration signals. Vibration is a crucial precursor to faults and failures in electrical machines, with frequency spectra in vibration signals providing vital information about the nature and severity of faults. Hence, representing both time and frequency makes spectrograms a logical choice in fault diagnosis for electrical machine systems.

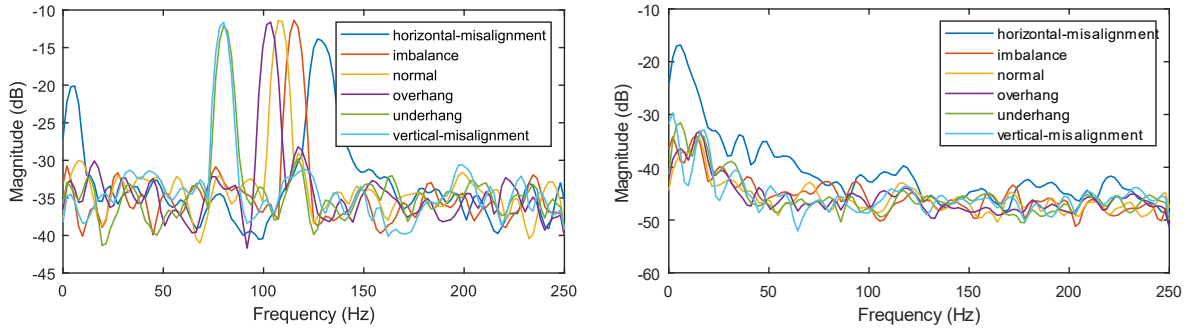

Figure 1. (a) The PSD estimation of the vibration signal on Location 1 and (b) Location 2 for each class

The Fourier Transform is a fundamental approach to discerning a signal's frequency content, deriving the frequency spectrum of a continuous signal using (4).

$$X(\omega) = \int_{-\infty}^{\infty} x(t) e^{-j\omega t} dt \qquad (4)$$

where $x(t)$ is the time-dependent continuous signal, and $X(\omega)$ is the counterpart of $x(t)$ in the frequency domain. While Fourier Transform provides insights into the signal's frequencies, it lacks details about the occurrence time of each frequency component. When the frequency content by time is required to be analyzed, the STFT is one of the most preferred methods. Segmenting the signal into smaller time windows and applying the Fourier Transform after multiplying the signal by a window function, a frequency spectrum emerges. The signal then undergoes multiplication by the time-shifted version of the window function, yielding another frequency spectrum. This process spans the defined time duration of the signal. When the resulting frequency spectra, all of equal length, are arrayed as rows in a matrix, a comprehensive depiction of time-dependent frequency changes materializes. The STFT is as expressed in (5)

$$STFT(\omega, \tau) = \int_{-\infty}^{\infty} x(t) W(t-\tau) e^{-j\omega t} dt \qquad (5)$$

where τ is the time delay to slide the window function $W(t)$. For the discrete input signals, discrete-time FT is replaced by the FT and the rest of the procedures remain the same. Figure 2 visualizes the STFT processes [18].

The processes visualized in Figure 2 can be summarized as follows.

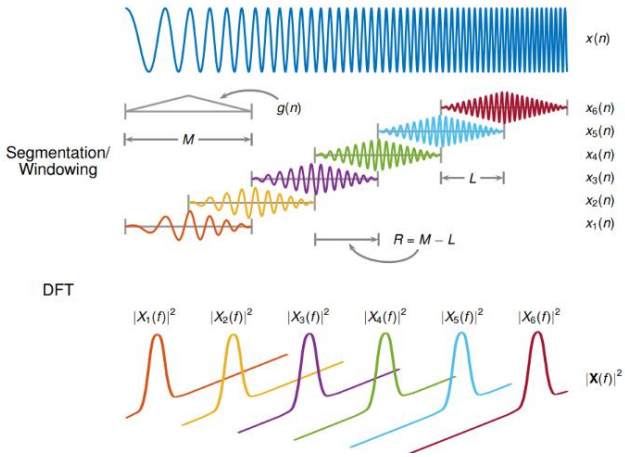

Figure 2. Visualization of STFT: segmentation, windowing, and DFT [18]

- The input signal is segmented, and each segment is multiplied by a proper window function of length.
- The window function slides over the input signal by L with $R = M - L$ samples overlap of consecutive segments.
- The frequency content of each segment is extracted by DFT and placed in the rows of a matrix. Thus, a 2D representation of the frequency by time change is obtained.

2.4. Scalogram

Much like a spectrogram, a scalogram visually illustrates how a signal's frequency changes over time. Unlike spectrograms, which rely on the Fourier Transform, scalograms based on the WT introduce a visually engaging exploration of time and frequency relationships.

In contrast to spectrograms, which offer a fixed time resolution through STFT, scalograms present a flexible narrative by balancing time and frequency resolutions. Unlike Fourier's sinusoidal signals, WT employs a mother function with distinct features. The signal to be analyzed is expressed

through this mother function, known for its irregularity, zero average, limited duration, and general asymmetry. Scalogram is obtained as a 2D representation of the input signal with the shifted and scaled variations of the mother function. While one of the dimensions is time, scale is the other one. Scale represents the mother function's different compressions or dilations, inversely related to frequency. While frequency increases, scale decreases, bringing about sharper time resolution. Conversely, a drop in frequency results in an increase in scale, widening the time window.

This tradeoff provides a zoom for detailed observation, enabling precise time resolution during sudden frequency changes and a high-frequency resolution within the domain of low-frequency elements. For a time-dependent continuous signal $x(t)$, Continuous Wavelet Transform (CWT) is expressed as in (6)

$$CWT(\tau,s) = \frac{1}{\sqrt{|s|}}\int_t x(t)\psi^*\left(\frac{t-\tau}{s}\right)dt \qquad (6)$$

where s is the scale referring to the compressions or dilations, τ is the time shift, $\psi(t)$ is a properly selected mother function. A mother function is required to be continuous, has null moments, and quickly decreases to zero with time (or band-limited). The admissibility condition to check any square-integrable candidate function is given in (7)

$$\int \frac{|\Psi(\omega)|^2}{|\omega|}d\omega < \infty \qquad (7)$$

where $\Psi(\omega)$ is the FT of the $\psi(t)$. When using CWT to create a scalogram, the procedures are similar to the ones to create spectrograms. The input signal is multiplied with $\psi^*(\tau,s)$ for different values of τ and s. While the time axis of the 2D scalogram is created by varying τ values, the scale axis corresponds to the different values of s. As previously mentioned, increasing the scale increases the time resolution and decreases the frequency resolution. The difference between CWT and STFT in terms of time and frequency resolution is visualized in Figure 3.

2.5. Classifiers

This study focuses on popular machine learning and deep learning methods as classifiers. While Decision Tree (DT), k-Nearest Neighbors (KNN), Support Vector Machine (SVM), and Linear Discriminant (LD) are preferred among the machine methods, Xception, InceptionV3, and MobileNet deep learning models have been meticulously chosen among Keras models, considering both dimension and performance metrics. Various fine-tuning strategies have been experimented upon the selected models to achieve the highest success.

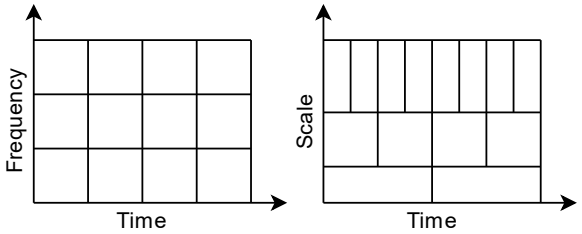

Figure 3 Decomposition of the time-frequency plane for (a) STFT and (b) CWT

3. Results and Discussion

The conducted study leverages vibration signals from an electrical machine system to classify mechanical faults within the system. 1-D power spectral density signals and 2-D scalogram and spectrogram images are created from the vibration signals. Machine learning techniques accept the power spectral density signals, while deep learning models use the scalogram and spectrogram images as inputs. Each machine learning algorithm was meticulously selected based on its proven effectiveness in handling similar datasets, ensuring a comprehensive evaluation of their performance in classifying mechanical faults. The deep learning models were chosen for their advanced capabilities in processing image data, leveraging transfer learning to enhance model accuracy and efficiency. The performances of the classifiers are evaluated with the well-accepted performance metrics explained in Table 2. The results reported in this study are obtained from the testing phase, utilizing a 5-fold cross-validation approach. This method involves dividing the dataset into five subsets, with each subset serving as a test set in turn, while the others are used for training. The performance metrics presented are the averages of the five folds.

In Table 2, True Positive (TP) refers to the number of examples correctly predicted as positive by the model, while True Negative (TN) is the number of examples correctly predicted as negative. False Positive (FP) represents the number of examples incorrectly predicted as positive but are negative, and False Negative (FN) is the number of examples incorrectly predicted as negative but are positive.

Table 2. The performance metrics

Metric	Description	Mathematical Expression
Accuracy (%)	The ratio of correctly classified instances to the total number of instances.	$\frac{TP}{TP+TN+FP+FN}$
Precision (%)	The ratio of true positive predictions to the total predicted positives.	$\frac{TP}{TP+FP}$
Recall (%)	The ratio of true positive predictions to the actual positives.	$\frac{TP}{TP+FN}$
F1 Score (%)	The harmonic mean of precision and recall.	$2 \times \frac{Precision \times Recall}{Precision + Recall}$

The performance of machine learning approaches is comparatively presented in Table 3. Table 3 provides a comparative overview of the performance of various classification methods applied to the dataset using accepted performance metrics. Moreover, the parameters yielding the best results are also provided. The learning parameters for the machine learning models were optimized using a random search strategy. For the Decision Tree classifier, the maximum number of splits was randomly selected from values between 4 and 100, with the optimal value chosen based on the highest accuracy. Various split rules, including the Gini's diversity index, twoing rule, and maximum deviance reduction, were evaluated. For the SVM classifier, linear, quadratic, and cubic kernels were tested, along with both one-vs-one and one-vs-all approaches for multiclass classification. Box constraint levels were randomly sampled from a range of 1 to 10. In the case of the KNN classifier, distance metrics such as Euclidean, cosine, Chebyshev, and Hamming were explored, and the number of neighbors was determined through random search from a range of 1 to 100. For Discriminant Analysis, both linear and quadratic kernels were considered, with covariance structures evaluated as full and diagonal. Among the examined methods, the KNN algorithm exhibited the highest performance with 96.56% accuracy, followed by SVM (95.85%) and DT (94.3%), while the LD method showed the lowest performance at 75.71%. These results highlight the non-linear nature of fault classes in the dataset and the effectiveness of algorithms like KNN in capturing complex patterns. The combination of PSD signal processing and KNN proves to be a robust method for fault detection in electrical machines. These findings underscore the importance of selecting an appropriate classification method tailored to the dataset for optimal performance. For a more detailed analysis of the classification performance of the methods, further information can be obtained through the analysis of confusion matrices provided in Figure 4 (a)-(d).

Table 3. Performance of Machine Learning approaches with PSD signals

Method	Parameters	Acc. (%)	Prec. (%)	Rec. (%)	F1 Score (%)
DT	max. # of splits: 100 split criterion: Gini diversity index	94.3	92.31	90.81	91.55
SVM	kernel function: linear box constraint level: 1 multiclass meth.: one vs one	95.85	94.18	95.98	95.08
KNN	# of neighbors: 1 distance metric: Euclidean distance weight: equal	96.56	96.75	96.72	96.74
LD	preset: Linear discriminant covariance structure: full	75.71	68.22	67.45	67.83

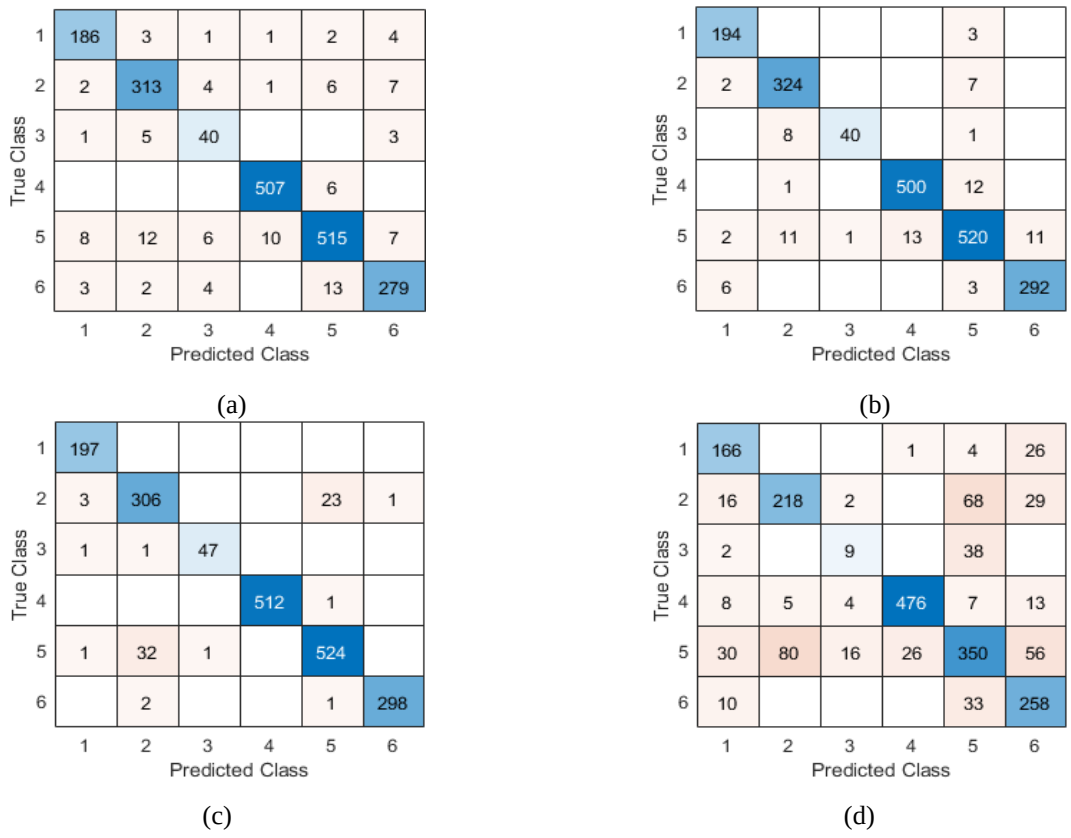

Figure 4. Confusion matrices for (a) DT, (b) SVM, (c) KNN, and (d) LD

Figure 4 shows that the KNN model demonstrates the most balanced and superior performance, particularly excelling in classifying 'normal', 'imbalance', and 'horizontal misalignment' categories, though it shows some confusion between 'overhang' and 'underhang' classes. SVM exhibits comparable performance to KNN but with slightly more errors in the 'vertical misalignment' class. While the DT model performs well overall, it struggles more with distinguishing between 'imbalance' and 'horizontal misalignment'. The LD model underperforms compared to the others, particularly in differentiating 'overhang' and 'underhang' classes, suggesting these fault types are not linearly separable. These results indicate that non-linear models, especially KNN and SVM, are more effective for fault detection.

As the second part of the study, deep learning models with the inputs of scalograms and spectrograms are analyzed using a transfer learning approach across three different models. The performances of Xception, InceptionV3, and MobileNet deep learning models are comparatively evaluated through heatmaps. The study presents how the performance of the methods changes with the fine-tuning and learning rate parameters. The learning rate has been optimized using a random search within the range of 5e-6 to 0.0002, and the fine-tuning steps have been selected from values between 10 and 200. The performance of each model for varying fine-tuning and learning rate parameters can be observed for the scalogram images in Figure 5 through the heatmaps provided.

Figure 5 illustrates the performance of three deep learning models (InceptionV3, Xception, and MobileNet) using scalogram inputs, represented as heatmaps across various fine-tuning steps and learning rates. The MobileNet architecture demonstrates superior performance, achieving a peak accuracy of 96.94% with 50 fine-tuning steps and a learning rate of 0.00002. InceptionV3 also exhibits robust performance, reaching 94.73% accuracy, while Xception shows comparatively lower performance.

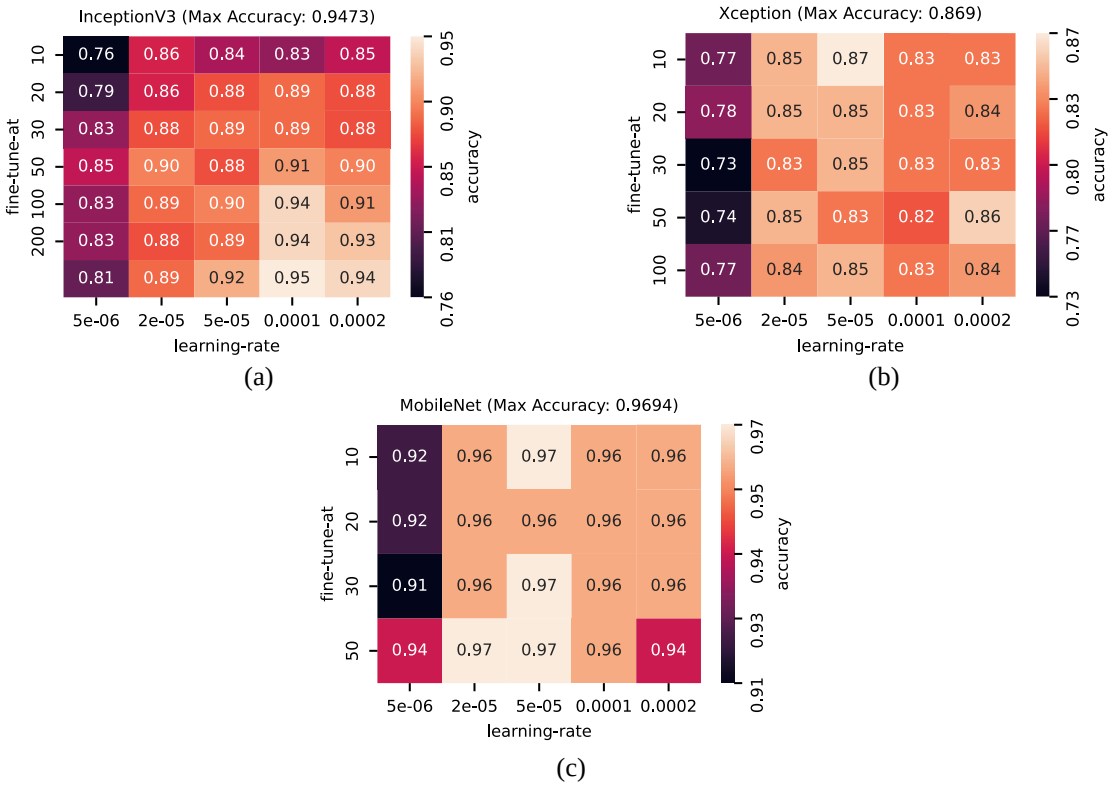

Figure 5. Heatmaps for the models (a) InceptionV3, (b) Xception, and (c) MobileNet with the scalogram images

These results suggest that the MobileNet architecture is particularly adept at extracting relevant features from scalogram representations of vibration signals for fault classification. Figure 6 displays the heat maps to indicate the effects of fine-tune-at and learning-rate parameters for the spectrogram images.

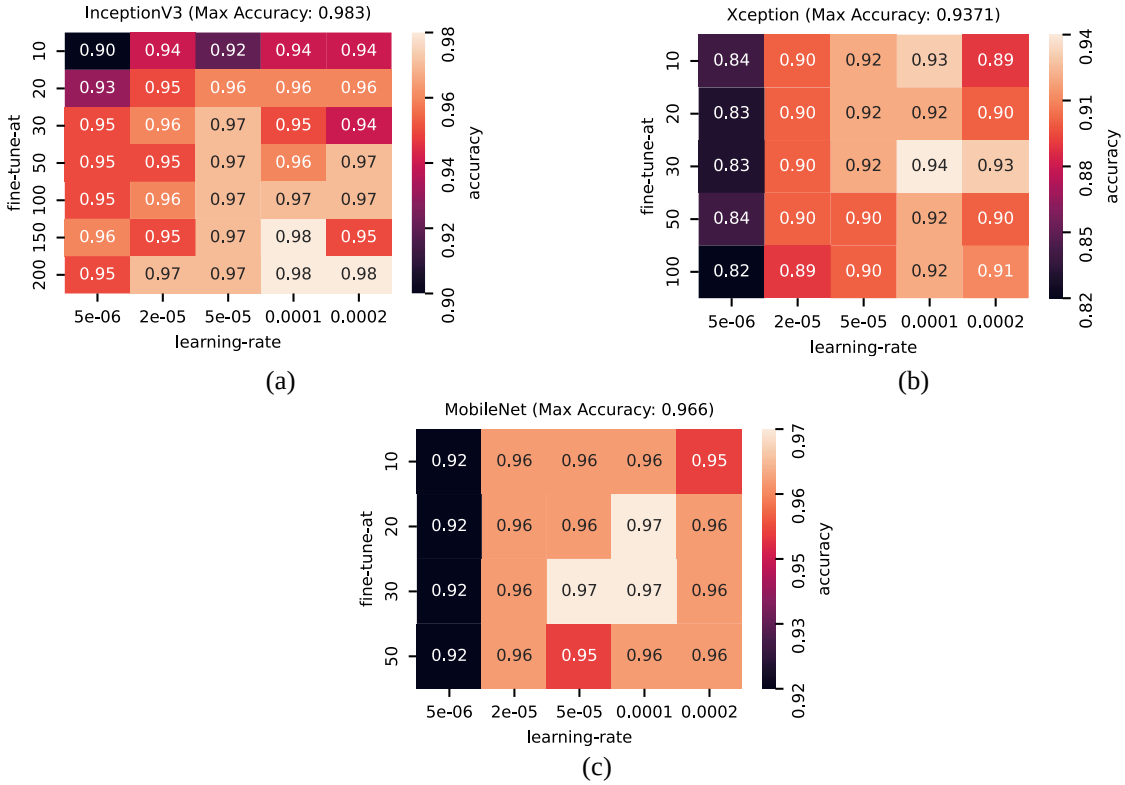

Figure 6. Heatmaps for the models (a) InceptionV3, (b) Xception, and (c) MobileNet with the spectrogram images

Figure 6 presents heatmaps depicting the performance of InceptionV3, Xception, and MobileNet models using spectrogram inputs across various fine-tuning steps and learning rates. Notably, the InceptionV3 model achieves the highest accuracy of 98.30% with 150 fine-tuning steps and a learning rate of 0.0001. Xception's performance significantly improves with spectrogram inputs compared to scalograms, while MobileNet maintains consistent performance. The superior results obtained with spectrogram inputs, particularly for InceptionV3, indicate that this time-frequency representation may capture fault-related features more effectively for the given dataset. The distinct optimal hyperparameter combinations for each model emphasize the necessity of model-specific tuning. These findings highlight the potential of deep learning approaches, especially InceptionV3 with spectrogram inputs, for highly accurate fault detection in electrical machinery.

Furthermore, our study underscores the necessity of selecting the most suitable model for different data representations, such as spectrograms and scalograms. For example, the InceptionV3 model outperforms MobileNet when processing spectrogram data, emphasizing the importance of evaluating the data type and model architecture features together.

Moreover, it's evident that the choice of learning rate significantly impacts the effectiveness of fine-tuning strategies. Carefully selecting the optimal learning rate tailored to each model and data type can substantially enhance accuracy rates. Table 4 summarizes the fine-tune-at and learning rate values where deep learning models achieve maximum accuracy.

In conducting a general assessment of our findings, we have compared the performance of traditional machine learning methods using PSD inputs with deep learning methods using spectrogram and scalogram inputs. While machine learning approaches have demonstrated strong performance, with KNN achieving the highest accuracy of 96.56% among PSD-based methods, deep learning models, particularly when using spectrogram inputs, have shown even higher accuracy. The InceptionV3 model with spectrogram inputs outperformed all other methods, achieving an impressive 98.30% accuracy. This suggests that hierarchical feature learning in deep neural networks is particularly effective for capturing complex patterns in vibration data for fault detection.

However, it's worth noting that the performance gap between the best machine learning model (KNN with PSD) and the best deep learning model (InceptionV3 with spectrograms) is relatively small (1.74%). This indicates that well-tuned traditional machine learning methods can still be competitive for fault detection tasks, especially when interpretability or computational resources are a concern. The choice between these approaches may depend on factors such as dataset size, need for interpretability, and available computational resources. Table 5 summarizes the best-performing models from each approach, highlighting their respective strengths in fault detection for electrical machinery.

Table 4. Performance of Transfer Learning models for scalogram and spectrogram images

Model	Scalogram images			Spectrogram images		
	Acc. (%)	fine-tuning step	learning rate	Acc. (%)	fine-tuning step	learning rate
InceptionV3	94.73	200	0.0001	98.30	150	0.0001
Xception	86.90	10	0.00005	93.71	30	0.0001
MobileNet	96.94	50	0.00002	96.60	30	0.00005

Table 5. Comparison of best-performing models for each approach

Approach	Model	Input	Acc. (%)	Prec.(%)	Rec. (%)	F1 score (%)
ML	KNN	PSD	96.56	96.75	96.72	96.74
ML	SVM	PSD	95.85	94.18	95.98	95.08
DL	InceptionV3	Spectrogram	98.30	98.10	98.44	98.56
DL	MobileNet	Scalogram	96.94	97.08	97.32	97.52

4. Conclusion and Suggestions

This study explores the performance of machine learning and deep learning models to classify the vibration data collected from electrical machines for fault detection. We first examine traditional machine learning methods like DT, KNN, SVM, and LD alongside three different deep learning models using transfer learning. The findings shed light on the effects of various data types and model architectures on classification performance.

Among the machine learning methods, which are fed by the 1-D PSD signal, the KNN model achieved the highest accuracy rate of 96.56%. On the other hand, the InceptionV3 deep learning model surpassed the highest accuracy with spectrogram images. The results highlight the importance of fine-tuning strategies, particularly emphasizing the significance of learning rate and fine-tune-at parameters. The InceptionV3 model has surpassed the others with an accuracy of 98.30% by selecting the fine-tune-at and learning rate parameters as 150 and 0.0001. The outcomes of the study can guide data analysis and fault diagnosis processes in industrial systems.

Acknowledgment

This work was supported by TUBITAK 1507 under grant number 7220463.

Contributions of the authors

Yunus Emre Acar: Conceptualization, Methodology, Software, Investigation, Writing, Visualization, Supervision.

Mehmet Emin KILIC: Project administration, Funding acquisition, Methodology, Software, Investigation, Writing, Visualization.

Conflict of Interest Statement

There is no conflict of interest between the authors.

Statement of Research and Publication Ethics

The study is complied with research and publication ethics.

References

[1] R. Hu, J. Wang, A. R. Mills, E. Chong, and Z. Sun, "Current-residual-based stator interturn fault detection in permanent magnet machines," *IEEE Transactions on Industrial Electronics*, vol. 68, no. 1, pp. 59–69, 2020.

[2] P. Nunes, J. Santos, and E. Rocha, "Challenges in predictive maintenance–A review," *CIRP Journal of Manufacturing Science and Technology*, vol. 40, pp. 53–67, 2023.

[3] G. A. Susto, A. Schirru, S. Pampuri, S. McLoone, and A. Beghi, "Machine learning for predictive maintenance: A multiple classifier approach," *IEEE Transactions on Industrial Informatics*, vol. 11, no. 3, pp. 812–820, 2014.

[4] S. Selcuk, "Predictive maintenance, its implementation and latest trends," *Proceedings of the Institution of Mechanical Engineers, Part B: Journal of Engineering Manufacture*, vol. 231, no. 9, pp. 1670–1679, 2017.

[5] Y. Ran, X. Zhou, P. Lin, Y. Wen, and R. Deng, "A survey of predictive maintenance: Systems, purposes and approaches," *arXiv preprint arXiv:1912.07383*, 2019.

[6] T. D. Popescu, D. Aiordachioaie, and A. Culea-Florescu, "Basic tools for vibration analysis with applications to predictive maintenance of rotating machines: an overview," *The International Journal of Advanced Manufacturing Technology*, pp. 1–17, 2022.

[7] N. Vafaei, R. A. Ribeiro, and L. M. Camarinha-Matos, "Fuzzy early warning systems for condition based maintenance," *Computers & Industrial Engineering*, vol. 128, pp. 736–746, 2019.

[8] G. Niu, X. Dong, and Y. Chen, "Motor Fault Diagnostics Based on Current Signatures: A Review," *IEEE Transactions on Instrumentation and Measurement*, 2023.

[9] F. Al-Badour, M. Sunar, and L. Cheded, "Vibration analysis of rotating machinery using time–frequency analysis and wavelet techniques," *Mechanical Systems and Signal Processing*, vol. 25, no. 6, pp. 2083–2101, 2011.

[10] J. R. Rivera-Guillen, J. De Santiago-Perez, J. P. Amezquita-Sanchez, M. Valtierra-Rodriguez, and R. J. Romero-Troncoso, "Enhanced FFT-based method for incipient broken rotor bar detection in induction motors during the startup transient," *Measurement*, vol. 124, pp. 277–285, 2018.

[11] J. Dalzochio et al., "Machine learning and reasoning for predictive maintenance in Industry 4.0: Current status and challenges," *Computers in Industry*, vol. 123, p. 103298, 2020.

[12] M. C. Garcia, M. A. Sanz-Bobi, and J. Del Pico, "SIMAP: Intelligent System for Predictive Maintenance: Application to the health condition monitoring of a wind turbine gearbox," *Computers in Industry*, vol. 57, no. 6, pp. 552–568, 2006.

[13] F. Ribeiro, "MaFaulDa-machinery fault database," *Signals, Multimedia, and Telecommunications Laboratory*, 2016.

[14] R. López-Valcarce, "General form of the power spectral density of multicarrier signals," *IEEE Communications Letters*, vol. 26, no. 8, pp. 1755–1759, 2022.

[15] L. Niu and F. Li, "Cooperative Spectrum Sensing for Internet of Things Using Modeling of Power-Spectral-Density Estimation Errors," *IEEE Internet of Things Journal*, vol. 9, no. 10, pp. 7802–7814, 2021.

[16] Z. Zhao, K. Peng, R. Xian, and X. Zhang, "Localization of Oscillation Source in DC Distribution Network Based on Power Spectral Density," *Journal of Modern Power Systems and Clean Energy*, vol. 11, no. 1, pp. 156–167, 2023.

[17] S. Benkner, A. Herzog, S. Klir, W. D. Van Driel, and T. Q. Khanh, "Advancements in Spectral Power Distribution Modeling of Light-Emitting Diodes," *IEEE Access*, vol. 10, pp. 83612–83619, 2022.

[18] "Signal Processing Toolbox," The MathWorks Inc., Available: https://www.mathworks.com/help/signal/ug/spectrogram-computation-with-signal-processing-toolbox.html (accessed February 1, 2024).